Assembly and Disassembly of Magnetic Mobile Micro-Robots towards 2-D Reconfigurable Micro-Systems

Chytra Pawashe*, Steven Floyd*, and Metin Sitti[†]

Abstract A primary challenge in the field of reconfigurable robotics is scaling down the size of individual robotic modules. We present a novel set of permanent magnet modules that are 900 μm $\times$ 900 μm $\times$ 270 μm in size, called Mag-μMods, for use in a reconfigurable micro-system. The module is actuated by oscillating external magnetic fields less than 5 mT in strength, and is capable of locomoting on a 2-D surface. Multiple modules can be controlled by using an electrostatic anchoring surface, which can selectively prevent specific modules from being driven by the external field while allowing others to move freely. We address the challenges of both assembling and disassembling two modules. Assembly is performed by bringing two modules sufficiently close that their magnetic attraction causes them to combine. Disassembly is performed by electrostatically anchoring one module to the surface, and applying magnetic forces or torques from external sources to separate the unanchored module.

1 Introduction

The field of reconfigurable robotics proposes versatile robots that can reconfigure into various configurations depending on the task at hand [1]. These types of robotic systems consist of many independent and often identical modules, each capable of motion, and capable of combining with other modules to create assemblies. These modules can then be disassembled and reassembled into alternate configurations. For example, Shen et al. [2] demonstrate SuperBot; this robot consists of 20 modules that can combine to form a mobile mechanism that can roll across the ground for 1 km and then reconfigure into one that can climb obstacles.

Another concept in the field of reconfigurable robotics is *programmable smart matter*, which is matter that can assemble and reconfigure into arbitrary three-dimensional (3-D) shapes, giving rise to *synthetic reality* [3]. This is similar to virtual or augmented reality, where a computer can generate and modify an arbitrary object. However, in *synthetic reality*, this object has physical realization. A primary

*Equally contributing co-authors

[†]Correspondence can be made to: Metin Sitti
Carnegie Mellon University, Dept. Mechanical Engineering
5000 Forbes Ave, Pittsburgh, PA 15213, USA
e-mail: sitti@cmu.edu

goal for programmable matter is scaling down the size of each individual module, with the aim of increasing spatial resolution of the final assembled product. Currently, the smallest actuated module in a reconfigurable robotic system fits inside a 2 cm cube [4], which is a self-contained module that is actuated using shape memory alloy. Scaling down further into the sub-millimeter scale brings new issues, including module fabrication, control, and communication. Micro-robotics technologies of the past few years have been progressing, with the introduction of untethered mobile micro-robots under 1 mm in size; these robots can potentially be used as micron-scale modules. The micro-robots that operate on two-dimensional (2-D) surfaces in the literature can be controlled either electrostatically [5], electromagnetically [6, 7], or using laser thermal excitation [8]. 3-D swimming micro-robots are also possible, and are often electromagnetically controlled [9, 10], and can even be powered by bacteria [10, 11].

For the purposes of micron-scale assembly using micro-robots, Donald et al. [5] demonstrate the assembly of four MEMS-fabricated silicon micro-robots, each under 300 μm in all dimensions, actuated by electric fields. Once assembled however, they cannot detach and reconfigure, because the electrostatic driving fields do not allow for disassembly. As a result, disassembling micron-scale modules is currently an unsolved problem.

2 Concept: Reconfigurable Micro-Robotics

In this work, we propose using sub-millimeter untethered permanent magnet micro-robots (Mag-μBots) actuated by external magnetic fields [6] as components of magnetic micro-modules (Mag-μMods), for creating deterministic reconfigurable 2-D micro-assemblies; this implies that the Mag-μMods will be able to both assemble and disassemble. Permanent magnet modules will attract each other with large magnetic forces, therefore it is necessary to reduce this inter-magnet force to facilitate disassembly. This is done by adding an outer shell to the Mag-μBot for the design of a module. The outer shell prevents two magnetic modules from coming into close contact, where magnetic forces will become restrictively high. A schematic of a Mag-μMod is illustrated in Fig. 1(a).

Motion of multiple Mag-μMods is achieved by employing a surface divided into a grid of cells, where each cell on the surface contains an addressable electrostatic trap capable of anchoring individual Mag-μMods to the surface and preventing them from moving. Unanchored Mag-μMods can move on the surface due to the imposed magnetic fields, and move in parallel. This technique is identical to controlling multiple Mag-μBots, explained in detail in [12]. Assembling two Mag-μMods is straightforward - by moving an unanchored Mag-μMod towards an anchored one, magnetic forces eventually dominate and cause the two Mag-μMods to self-assemble.

Disassembling two Mag-μMods is problematic. For this to occur, the magnetic force between two Mag-μMods must be overcome and the two separated without

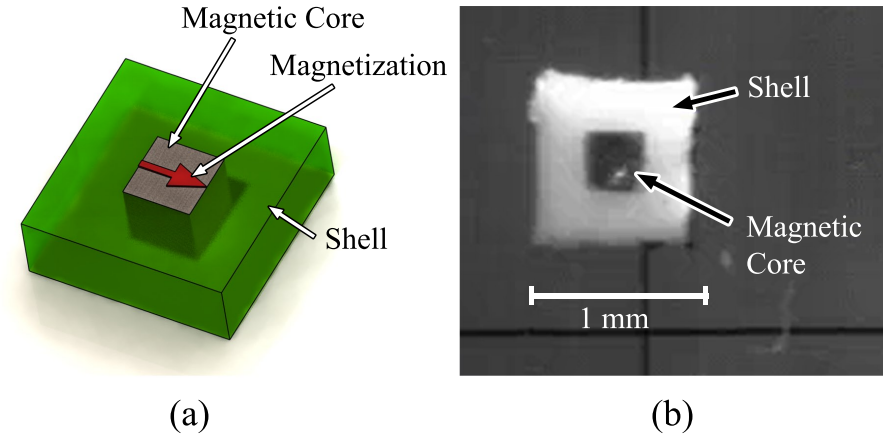

Fig. 1 (a) Schematic of a Mag-μMod. A permanent magnetic core with indicated magnetization is surrounded by a magnetically inactive shell. (b) Photograph of a Mag-μMod. A 300 $\times$ 300 $\times$ 170 μm^3 Mag-μBot is used as the magnetic core of the module, with a polyurethane shell 900 μm $\times$ 900 μm $\times$ 270 μm in outer dimensions surrounding the core.

physically contacting either one. To do this, we use the electrostatic grid surface to anchor parts of assembled modules, and examine the effectiveness of both externally applied magnetic forces and torques to disassemble unanchored modules on the assembly.

Figure 2 displays the concept of multiple Mag-μMods assembling, disassembling, and reconfiguring into different configurations. Because the Mag-μMods are magnetic, they can only assemble into configurations that are magnetically stable.

3 Experimental Setup, Operation, and Fabrication

Mag-μBots are actuated by six independent electromagnetic coils, aligned to the faces of a cube approximately 11 cm on a side, with horizontal and vertical coils capable of producing maximum field strengths at the position of the Mag-μBot (see Fig. 3) of 3.0 mT and 2.3 mT, respectively. Control of the electromagnetic coils is performed by a PC with a data acquisition system at a control bandwidth of 1 kHz, and the coils are powered by custom-made electronic amplifiers.

Actuation of each Mag-μBot is accomplished by using two or three electromagnetic coils. One or more horizontal coils are first enabled (coil D in Fig. 3), causing the Mag-μBot to orient in the direction of the net magnetic field. The magnetic force exerted by the coils on the Mag-μBot is insufficient to translate it, due to friction from the surface. Thus, vertical clamping coils (coils C and F in Fig. 3) are enabled and pulsed using a sawtooth waveform. This results in a non-uniform rocking motion of the Mag-μBot, which induces stick-slip motion across the surface. In general, the Mag-μBot's velocity increases with pulsing frequency, typically from

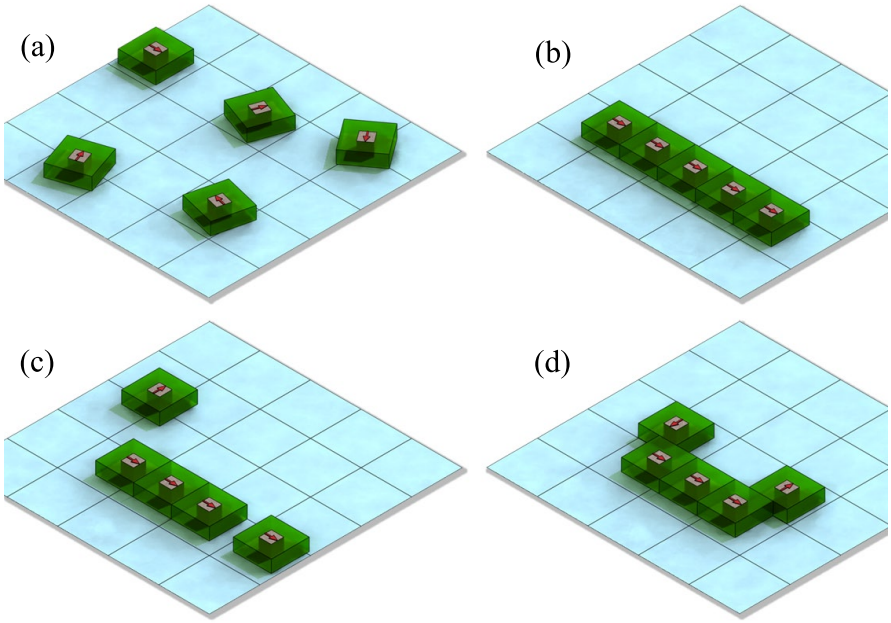

Fig. 2 Schematic of five Mag-μMods operating on an electrostatic grid surface, where each cell can be individually activated to anchor-down individual Mag-μMods; unanchored Mag-μMods can be moved by the global magnetic field. (a) The five Mag-μMods are separate, and (b) assemble into a magnetically-stable line. In (c), the two outer Mag-μMods disassemble from the line, and (d) reconfigure into a magnetically stable 'U' shape.

1-100 Hz, and can exceed velocities of 16 mm/s in air. The Mag-μBot is also capable of operating in fluids of viscosities less than about 50 cSt, and can operate on a variety of smooth and rough magnetically inactive surfaces, provided that the adhesion between the Mag-μBot and surface is low. Further explanation of this system is discussed in [6, 12, 13] and demonstration movies can be found online at [14].

3.1 Mag-μBot and Mag-μMod Fabrication

Mag-μBots can be produced in a batch process using soft-lithography techniques in a manner similar to [15]. The Mag-μBot used in this work is rectilinear, 300 $\times$ 300 $\times$ 170 μm^3, and is composed of a mixture of neodymium-iron-boron (NdFeB) particles (Magnequench MQP-15-7, refined in a ball mill to produce particles under 2 μm in size) suspended in a polyurethane (TC-892, BJB enterprises) matrix. The fabrication process used is shown in Fig. 4.

A Mag-μMod is a polyurethane shell encasing a magnetic core, the Mag-μBot. The shells are fabricated in a manner similar to the Mag-μBot, omitting the addition

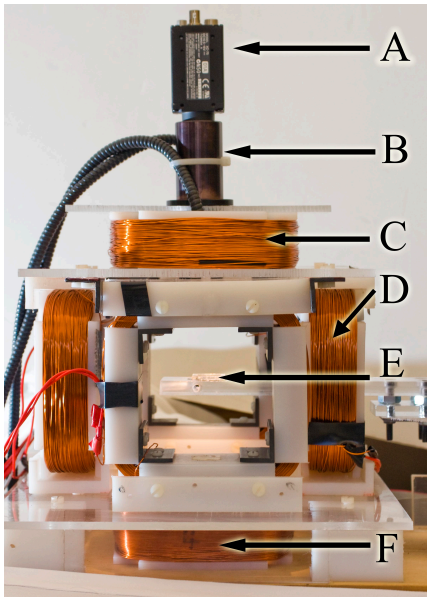

Fig. 3 Photograph of the electromagnetic coil setup, where A is the camera for visual feedback, B is the microscope lens, C is the top coil, D is one of four upright coils that orients the Mag-μBot within the plane on the surface, E is the surface on which the Mag-μBot locomotes, and F is the bottom coil. The top and bottom coils are clamping coils, which provide a clamping force and a torque that pushes and orients the Mag-μBot towards the surface, respectively.

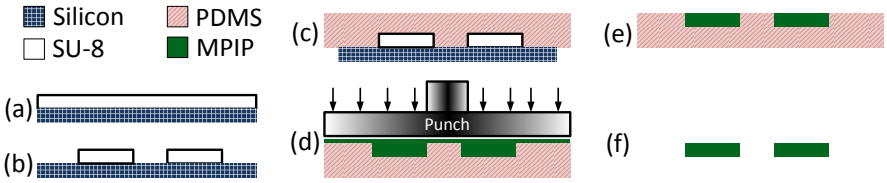

Fig. 4 The fabrication steps used to batch manufacture polymer Mag-μBots. (a) SU-8 is spin coated onto a silicon wafer to the desired thickness of the final micro-robot, and (b) is patterned and hardened to create the positive mold. (c) Polydimethylsiloxane (PDMS, Dow Corning HS II RTV) mold making material is poured onto the positive mold and allowed to cure. (d) The PDMS is removed from the positive mold, creating the negative mold, and a mixture of magnetic-powder-impregnated polyurethane (MPIP) is prepared by mixing 4 parts NdFeB powder to 1 part polyurethane, degassed in a vacuum, and then poured onto the PDMS mold. A large permanent magnet (not shown) is placed under the PDMS mold to ensure the NdFeB powder is densely packed in the mold. After a second degassing, a polypropylene flat punch is pressed and held against the mold, which pushes excess NdFeB-polyurethane out, leaving a thin backing layer. Next, the large magnet is moved to the front of the mold so that the NdFeB particles will orient along the lengths of the Mag-μBots, facilitating a higher net magnetization in the length-wise direction, as magnetic domains will be more favorably oriented. (e) After hardening and removing the punch, excess polyurethane is peeled off manually using tweezers. (f) Finished polymer Mag-μBots can be easily removed from the mold with tweezers or micro-probes, and are later magnetized in a 1 T magnetizing field along its length. This results in a magnetization of about 58 kA/m, estimated from measurements using a vibrating sample magnetometer (ADE Technologies Inc.).

of NdFeB powder into the mold mixture and the magnetization step. Assembly of the Mag-μBot into a shell is performed manually using tweezers under an optical microscope, and the two components are held together by a pressure-fit (an adhesive can also be used to bind the two components). Figure 1(b) displays an assembled Mag-μMod. In the presence of the global magnetic fields, these modules move similarly to individual Mag-μBots without shells, exhibiting stick-slip motion across the working surface, however at lower velocities of about 0.5 mm/s.

3.2 Electrostatic Grid Surface Fabrication

The electrostatic grid surface, described in [12], is necessary to enable the control of multiple Mag-μBots or Mag-μMods. It consists of an array of independently addressable pads, each pad containing a set of interdigitated electrodes to generate high electric fields. The surface is fabricated with the steps shown in Fig. 5. Mag-μMods are placed on this surface and are operated in a low-viscosity silicone oil (Dow Corning 200 fluid, 20 cSt) which supports the generation of the large electric fields required to anchor individual Mag-μMods. Anchoring occurs through a capacitive coupling force to the surface for conductive materials.

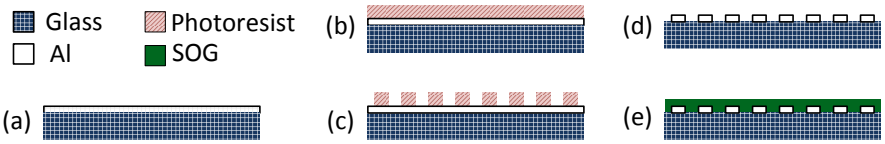

Fig. 5 Steps for fabricating an interdigitated electrostatic anchoring surface used for the control of multiple Mag-μMods. (a) 100 nm of aluminum is sputtered onto a glass substrate. (b) Photoresist is spun onto the metal surface, and patterned in (c) with a spacing of 10 μm. The aluminum layer is etched in (d) to create the interdigitaded electrode pattern. For this work, four 2 mm $\times$ 2 mm electrode pads are patterned in a 2 $\times$ 2 grid configuration. After creating interconnects from the electrodes to external electronics (not shown), a 400 nm spin-on glass (SOG) insulation layer is deposited in (e). Mag-μMods operate directly on this spin-on glass surface.

4 Modeling

Each of the Mag-μMods is subject to magnetic forces created by the driving magnetic field and other Mag-μMods, electrostatic anchoring forces created by the grid surface, and surface forces such as adhesion and friction. In this section, these different forces are briefly modeled to provide insight to their relative magnitude and effect on both assembly and disassembly of Mag-μMods.

4.1 Magnetic Influences

Each magnetized Mag-μMod and each electromagnet creates a magnetic field: $B_{mr}(x,y,z)$ and $B_{ec}(z)$, respectively. Within these magnetic fields, magnetized Mag-μMods experience both a torque and a force. This magnetic torque is proportional to the magnetic field strength, and acts to bring the internal magnetization of the Mag-μMod into alignment with the field. Magnetic force is proportional to the gradient of the magnetic field, and acts to move Mag-μMods to a local maximum. The relations that govern these interactions are:

$$\mathbf{T}_m = V_m \mathbf{M} \times \mathbf{B}(x,y,z) \tag{1}$$

$$\mathbf{F}_m = V_m (\mathbf{M} \bullet \nabla) \mathbf{B}(x,y,z) \tag{2}$$

where $\mathbf{T}_m$ is the torque the Mag-μMod experiences, V_m is the volume of the Mag-μMod's magnetic core, $\mathbf{M}$ is the magnetization of the Mag-μMod's magnetic core, and $\mathbf{F}_m$ is the force the Mag-μMod experiences.

To approximate the forces and torques Mag-μMods exert on each other, they are modeled as magnetic dipoles, located at their geometric center, with a value equal to their core's magnetic moment. Due to the symmetry inherent in this approximation, it is convenient to describe the field produced by the Mag-μMod's core in spherical coordinates:

$$\mathbf{B_{mr}}(r,\theta) = \frac{\mu_0}{4\pi} V_m \mathbf{M} \left(\frac{2cos(\theta)}{r^3} \mathbf{e}_r + \frac{sin(\theta)}{r^3} \mathbf{e}_\theta \right) \tag{3}$$

where $\mu_0 = 4\pi \times 10^{-7}$ H/m is the permeability of free space, $M = 58$ kA/m is the estimated magnetization of each Mag-μBot, $\mathbf{e}_r$ is a unit vector aligned with the magnetization of the Mag-μBot, $\mathbf{e}_\theta$ is a unit vector representing rotations about the y-axis, r is the distance from the center of the Mag-μMod, and θ is the azimuthal angle. Coordinate conventions are shown in Fig. 6. The attractive force that arises between two aligned Mag-μMods when separated by a distance r is:

$$F_{mr}(r) = \frac{\mu_0}{4\pi} (V_m M)^2 \frac{6}{r^4} \tag{4}$$

The magnetic field created by each of the electromagnets is directed towards the coil and is experienced by all Mag-μMods:

$$B_{ec}(z') \approx \frac{\mu_0 N I a^2}{2(z'^2 + a^2)^{3/2}} = 9.49 \times 10^{-4} (I) \left[\frac{\mathrm{T}}{\mathrm{A}} \right] \tag{5}$$

where, $z' = 0.095$ m is the approximate distance from the center of an electromagnet to the workspace, $N = 510$ is the number of turns, I is the current flowing through it, and $a = 0.0695$ m is its characteristic radius [16]. From this, the gradient produced by a single electromagnet can be derived:

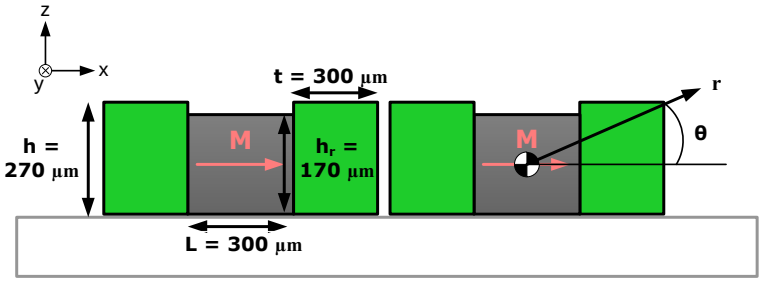

Fig. 6 Side view cross-section schematic of two Mag-μMods. Relevant geometry and coordinates used in equations are shown.

$$\left|\Delta B_{ec}(z')\right| \approx \frac{3\mu_0 NIa^2 z'}{2(z'^2+a^2)^{5/2}} = 1.95\times10^{-2}(I)\left[\frac{\mathrm{T}}{\mathrm{A\cdot m}}\right] \tag{6}$$

If two electromagnets are used in opposition, the combined field gradient is larger:

$$\left|\Delta B_{2ec}(z')\right| \approx \frac{\mu_0 NI}{2az'} = 4.85\times10^{-2}(I)\left[\frac{\mathrm{T}}{\mathrm{A\cdot m}}\right] \tag{7}$$

4.2 Electrostatic Influences

A conductive object with non-negligible surface roughness operating on an insulating surface covering a set of interdigitated electrodes at an applied voltage difference of V_{id} will assume a potential halfway between the two, or $\frac{1}{2}V_{id}$, if it overlaps equal areas of electrodes at both voltages; applicable when the electrode and gap widths (10 μm each) are much smaller than the length of the object (300 μm). For the conductive magnetic core of a Mag-μMod, its surface roughness traps a fluid layer with thickness comparable to the its maximum asperity height of about $b = 9$ μm beneath it, increasing the separation from the electrodes and causing the total capacitance C_{tot} between the Mag-μMod and the electrodes to be:

$$C_1 = \frac{\varepsilon_0\varepsilon_{r1}A_{id}}{g} \approx 3.48\times10^{-12}\ [\mathrm{F}] \tag{8}$$

$$C_2 = \frac{\varepsilon_0\varepsilon_{r2}A_{id}}{b} \approx 1.11\times10^{-13}\ [\mathrm{F}] \tag{9}$$

$$C_{tot} = \left(C_1^{-1}+C_2^{-1}\right)^{-1} \approx 1.07\times10^{-13}\ [\mathrm{F}] \tag{10}$$

where C_1 is the capacitance associated with the glass insulation layer, $\varepsilon_0 = 8.854\times10^{-12}$ F/m is the permittivity of free space, $\varepsilon_{r1} = 3.5$ is the relative permittivity of the glass surface, $A_{id} = 4.5\times10^{-8}$ m^2 is half the apparent area of the overlap between

the Mag-μMod's magnetic core and the electrodes, C_2 is associated with the fluid gap, and $\varepsilon_{r2} = 2.5$ is the relative permittivity of the silicone oil environment. Using the principal of virtual work, the electrostatic anchoring force with a fluid gap, F_e, will be:

$$F_e = \frac{1}{16} V_{id}^2 C_{tot}^2 \left[\frac{1}{C_1 g} k + \frac{1}{C_2 a} (1-k) \right] \geq 5.16 \times 10^{-10} (V_{id}^2) \left[\frac{\mathrm{N}}{\mathrm{V}^2} \right] \tag{11}$$

where k is an empirical constant ($0 < k < 1$) used to bound the solution space.

To anchor a Mag-μMod to the surface, the electrostatic anchoring force must suppress three effects: (1) out-of-plane rotations about an axis in the $x-y$ plane of the Mag-μMod from magnetic fields in the z-direction, (2) rotations within the plane of motion about the z-axis due to magnetic fields in the $x-y$ direction, and (3) translation due to magnetic field gradients in a direction in the $x-y$ plane.

During stick-slip locomotion, each Mag-μMod can experience fields of up to 4.82 mT when using multiple coils. This creates out-of-plane magnetic torques up to 4.28×10^{-9} N$\cdot$m on the Mag-μMod, which can be approximated as a pair of 14.3 μN forces acting in opposite directions on opposite sides of the Mag-μMod. To prevent this rotation, the electrostatic surface must exert double this force, or approximately 28.6 μN, applied at the centroid of the Mag-μMod. Using Eq. (11), this force requires $V_{id} = 235$ V applied to the electrostatic surface.

4.3 Surface Forces

While immersed in silicone oil, Mag-μMods experience reduced adhesion forces to the surface [17, 13] when compared to air. Adhesion to the surface while immersed in silicone oil can be taken to be negligible. Thus, the maximum friction force, $F_{f,max}$, experienced by a Mag-μMod is determined using a Coulomb friction relation:

$$F_{f,max} = \mu_f (W + F_e + F_m) \tag{12}$$

where μ_f is the coefficient of friction, W is the Mag-μMod's buoyant weight, F_e is any electrostatic anchoring force, and F_m is any magnetic force that pushes the Mag-μMod toward the surface. Based upon the densities of polyurethane (1140 kg/m^3) and NdFeB (7400 kg/m^3), and assuming close packing of NdFeB spheres, the effective density of a Mag-μMod is 5770 kg/m^3. When immersed in silicone oil (density 950 kg/m^3), the buoyant weight $W = 1.09$ μN. From empirical results in Sec. 7, $F_{f,max} = 228$ nN for a Mag-μMod, when $F_e = F_m = 0$; thus using Eq. (12), $\mu_f = 0.21$ in the experiments.

5 Mag-μMod Assembly

As two Mag-μMods approach each other, the forces and torques between them increase due to the r^3 dependence of their fields, from Eq. (3), and they will eventually combine into the configuration shown in Fig. 6. Using the dipole approximation (Eq. (4)), the distance where two Mag-μMods jump-into-contact can be estimated by determining when the inter-magnetic force overcomes the friction force, based upon the Mag-μMod's buoyant weight. Conversely, given the jump-into-contact distance, the friction coefficient can be estimated.

When two Mag-μMods are assembled, they are separated by two shells, each one approximately 300 μm thick; thus their center-to-center distance is approximately 900 μm. From Eq. (4), the mutual attractive force is 720 nN. The assembled structure can continue to locomote, as shown in Fig. 10(d).

6 Mag-μMod Disassembly

To disassemble two Mag-μMods that are assembled, the application of external magnetic forces, torques, or both may be utilized. In this work, three methods for disassembly are described, and the necessary forces and torques for disassembly, as well as necessary anchoring forces, are derived.

Method 1 - Translation Disassembly: To separate two assembled Mag-μMods by translating one away from another, one Mag-μMod must first be anchored to the surface. Next, the global magnetic field gradient acting upon the unanchored Mag-μMod must overcome the local magnetic field gradient created by the anchored Mag-μMod, and the friction force, shown in Fig. 7. From Sec. 5, two Mag-μMods have an attraction force of 720 nN. Combined with the friction force of 228 nN, the total lateral force which must be overcome is 948 nN, this corresponds to a necessary field gradient of 1.07 T/m from Eq. (2). To produce this gradient from a single coil in Fig. 3, 55 amps would have to be passed through an electromagnet (Eq. (6)). Alternatively, using two coils separated by 19 cm, 22 amps per coil (or 44 amps total) would be required (Eq. (7)).

The anchored Mag-μMod experiences forces from both the electromagnet and the other Mag-μMod, totaling 1.67 μN. This force must be balanced by a friction force to the surface, which ensures that this Mag-μMod remains stationary. Using a friction coefficient of $\mu_f = 0.21$ and Eq. (12), with $F_m = W = 0$ to attain a conservative estimate, $F_e > 7.94$ μN is necessary to remain stationary. This corresponds to $V_{id} > 124$ V (Eq. (11)).

Method 2 - In-Plane Rotation Disassembly: Applied magnetic torques can be used to separate two assembled Mag-μMods. As in Method 1, one of the Mag-μMods must be electrostatically anchored to remain stationary. Then, the in-plane magnetic field is rotated about the z-axis, twisting the unanchored Mag-μMod about its point of contact with the anchored Mag-μMod. The unanchored Mag-μMod is

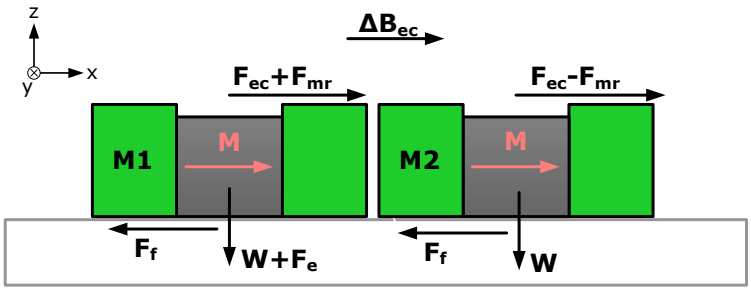

Fig. 7 Side view cross-section schematic of two Mag-μMods being disassembled via translation disassembly and the relevant forces from the electromagnetic coils (F_{ec}) and from other Mag-μMods (F_{mr}) acting upon them. M1 is anchored to the surface while M2 is pulled by the externally-induced field gradient ΔB_{ec}.

rotated until it is in a configuration with the anchored Mag-μMod that minimizes their attractive force. Once this orientation is achieved, the unanchored Mag-μMod can move away using its standard locomotion method using pulsed magnetic fields, leaving the anchored Mag-μMod in place. Fig. 8 displays a schematic of this disassembly technique.

The applied magnetic torque that rotates the unanchored Mag-μMod must overcome the torque created by the anchored Mag-μMod, which acts to align the two. This torque is calculated as a function of θ and ϕ as one Mag-μMod rotates about the other at a constant distance $r = 900$ μm, shown schematically in Fig. 8. Using Eqs. (1) and (3), the maximum torque is 2.16×10^{-10} N$\cdot$m, and occurs when $\theta = 0,\ \phi = [\pi/2, 3\pi/2]$. A weight-based friction torque of 5.13×10^{-11} N$\cdot$m, acting at the centroids of opposite sides of the Mag-μMod, is added to the magnetic torque, as it must too be overcome. To counteract this torque, using Eq. (5), a single electromagnet from Fig. 3 must impose a field of $B_{ec} = 301$ μT, which corresponds to $I = 0.32$ A.

To determine the necessary anchoring force, both the electromagnet's applied torque and the rotating Mag-μMod's torque are applied on the stationary Mag-μMod. To resist these moments, the electrostatic-based friction is treated as a force couple acting at the half body centroids of the Mag-μBot, as it is the only part of the Mag-μMod being pulled down. Each force in this force pair must exceed 3.22 μN, leading to a conservative total anchoring force of $F_e = 30.7$ μN that must be applied; from Eq. (11), $V_{id} = 244$ V.

Method 3 - Out-of-Plane Rotation Disassembly: Another approach for using applied torques to separate two Mag-μMods requires that one of the Mag-μMods be anchored to the surface, while the other Mag-μMod is unanchored and rotated about an axis in the $x-y$ plane, shown schematically in Fig. 9. The unanchored Mag-μMod rotates until the mutual attractive force between the two Mag-μMods is minimized, or becomes repulsive. When this orientation achieved, the unanchored Mag-μMods can move away using its standard locomotion method.

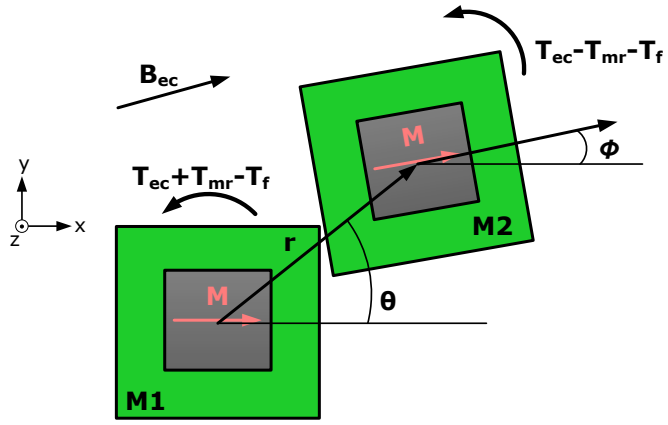

Fig. 8 Top view schematic of two Mag-μMods being disassembled via in-plane rotation disassembly, and the relevant torques from the electromagnetic coils (T_{ec}), from other Mag-μMods (T_{mr}), and from friction (T_f) acting upon them. M1 is anchored to the surface while M2 is disassembled by rotating it using the global electromagnet-induced field (B_{ec}).

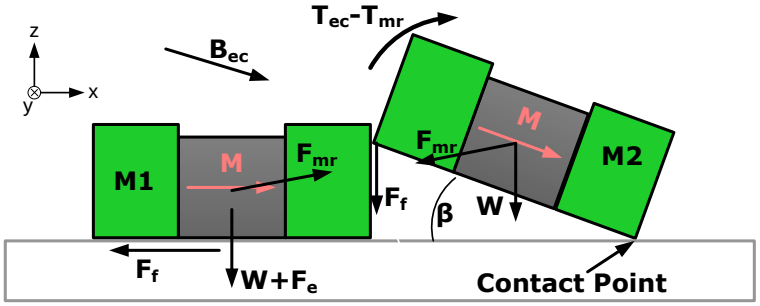

Fig. 9 Side view cross-section schematic of two Mag-μMods being disassembled via out-of-plane rotation disassembly, the relevant torques from the electromagnetic coils (T_{ec}), from other Mag-μMods (T_{mr}), and the friction forces (F_f) acting upon them. M1 is anchored to the surface while M2 is disassembled by rotating it using the global electromagnet-induced field (B_{ec}).

Assuming that the point of contact for the rotating Mag-μMod remains fixed (see Fig. 9), the maximum torque required to rotate it upward is 7.98×10^{-10} N$\cdot$m, and occurs at an angle of $\beta = 11.5°$. This torque is a function of the magnetic force and torque exerted on the unanchored Mag-μMod by the anchored Mag-μMod (see Eqs. (1), (2) and (3)), the weight, and the contact friction between the two (see Eqs. (4) and (12)). After passing a critical angle, $\beta_{crit} = 69.3°$, the force between the two Mag-μMods becomes repulsive.

To overcome this maximum torque, a single electromagnet has to produce a field of $B_{ec} = 899\ \mu T$ using Eq. (5), implying $I = 0.95$ A. For electrostatic anchoring to effectively resist the torques from both the magnetic field and the moving Mag-

μMod, a force of $F_e = 10.6$ μN must be applied with $V_{id} = 144$ V from Eq. (11).

7 Experimental Results and Discussion

In the experiments, two Mag-μMods are placed on an electrostatic grid surface with four anchoring pads, in a 2×2 configuration, and operated in a silicone oil environment. Motion is achieved by pulsing the electromagnetic coils from 1-3 Hz using a sawtooth waveform. An anchoring voltage of $V_{id} = 400$ V is used, which is greater than any of the estimated requirements presented in Sec. 6, and ensures proper anchoring. Movies of assembly and disassembly can be found online [14].

Assembly: The process of Mag-μMods assembling is demonstrated in Fig. 10. In this experiment, the magnetic attraction between the Mag-μMods is sufficient to combine them when their center to center distance is 1.2 mm. Using Eq. (4), This corresponds to an attractive force of 228 nN. The assembled Mag-μMod structure is capable of motion, shown in Fig. 10(d).

Two Mag-μMods can also combine in 3-D when one slides over the other, resulting in a cuboid structure. In this configuration, the Mag-μMods are much closer than the case in Fig. 10, and as a result are held together with a greater force. Disassembly techniques for this 3-D configuration will be investigated in future works.

Method 1 - Translation Disassembly: Fig. 11 demonstrates two Mag-μMods being disassembled. Due to hardware limitations of the electromagnetic coil system, a permanent NdFeB magnet $6.3 \times 6.3 \times 31.8$ mm^3 (N42 grade, magnetized along its length) was placed approximately 1.5 cm from the workspace, and is used to generate the necessary large magnetic field gradient. When the permanent magnet is brought near the workspace, its field gradient exceeds that of the anchored Mag-μMod, forcing the unanchored Mag-μMod to separate.

Method 2 - In-Plane Rotation Disassembly: Disassembly of two Mag-μMods using torques exerted by the electromagnetic coils is demonstrated in Fig. 12. One Mag-μMod is electrostatically anchored while the other is rotated about the z-axis to minimize the attractive force. Once in a configuration with nearly zero attractive force between them ($\theta = \pi/2$, $\phi = \pi/2$ using the convention of Fig. 8), the unanchored Mag-μMod is moved away from the anchored Mag-μMod using a standard locomotion signal from the electromagnets.

Method 3 - Out-of-Plane Rotation Disassembly: In Fig. 13, a magnetic field was created by placing a 1.27 cm cube-shaped NdFeB (grade N42) permanent magnet approximately 9 cm beneath the surface, and the unanchored Mag-μMod rotated out-of-plane about its contact point with the surface. When the angle of rotation is sufficiently large, the force between the two two Mag-μMods becomes repulsive, and the unanchored Mag-μMod can be disassembled by moving it away with a stan-

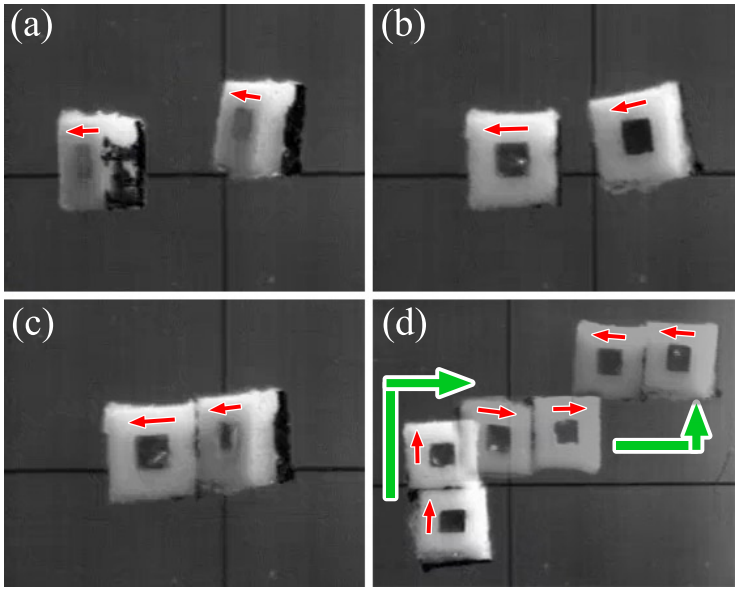

Fig. 10 Frames from a video of two Mag-μMods assembling; arrows on Mag-μMods indicate magnetization direction. In (a), the Mag-μMods are initially separated, and oriented towards the surface by the electromagnetic clamping field, which is turned off in (b). The Mag-μMods attract each other and assemble in (c). The assembled Mag-μMods move together in (d), shown as superimposed frames.

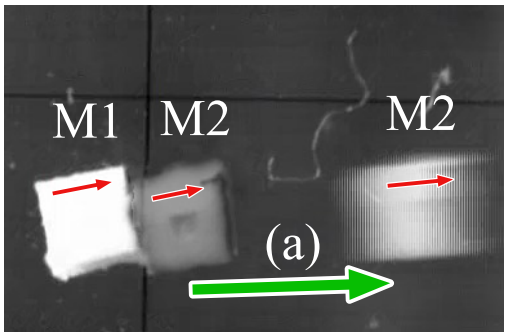

Fig. 11 Superimposed frames from a video of two Mag-μMods, M1 and M2, disassembling by manually bringing in a strong permanent magnet to the right of the image. M1 and M2 are initially assembled, and M1 is anchored. M2 disassembles in (a) when the permanent magnet is sufficiently close to the working area.

dard locomotion signal from the electromagnets.

From the three methods of disassembly, *Method 2 - In-Plane Rotation Disassembly*, is advantageous because only small magnetic fields are required, which can be created by the electromagnetic coils used to locomote the Mag-μMods. *Method 1 - Translation Disassembly* requires a large field gradient, which must currently be produced by an external permanent magnet. While *Method 3 - Out-of-Plane Rotation Disassembly* should be possible with the current electromagnetic system, successful disassembly occurred intermittently, implying that the necessary fields can

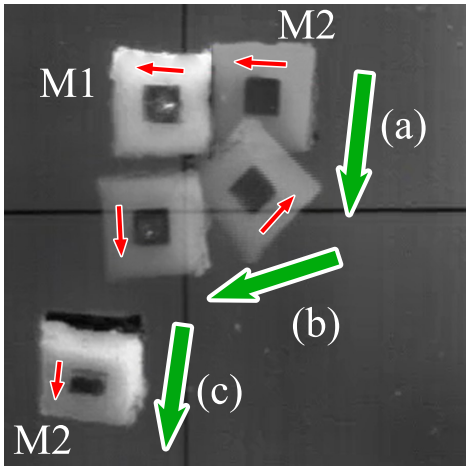

Fig. 12 Superimposed frames from a video of two Mag-μMods, M1 and M2, disassembling by using applied electromagnetic torques from the electromagnetic coils. M1 is anchored to the surface and initially combined with M2. The external fields are applied and cause M2 to orient downwards from (a) to (b) by rotating it clockwise. In this configuration, M2 can walk away from M1 in (c), as the two modules repel each other.

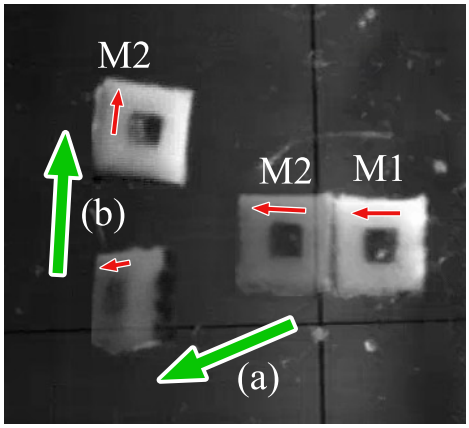

Fig. 13 Superimposed frames from a video of two Mag-μMods, M1 and M2, disassembling by manually bringing permanent magnet below the surface, with magnetization pointing into the page. M1 and M2 are initially assembled, and M1 is anchored. A leftward driving field is initially applied, and M2 disassembles in (a) when the permanent magnet is positioned. M2 then moves upwards in (b).

be significantly larger than estimated. For assured success, a permanent magnet was used in Methods 1 and 3, though placed much further away for Method 3.

These permanent magnets can potentially be replaced by high-field electromagnetic coils to support future automation at the cost of increasing the complexity of the electromagnetic coil system. On the other hand, Methods 1 and 3 require fewer magnetic field direction changes, and can potentially be quicker and more reliable than Method 2 for disassembly. Method 3 in particular can be implemented by a single high-field coil placed underneath the working surface, only marginally increasing complexity of the system.

8 Conclusion

In this study, robotic magnetic micro-modules, under 1 mm in size, have been shown to assemble and disassemble by using externally applied electromagnetic fields and electrostatic anchoring techniques. Future work will include extending this concept to larger numbers of modules, demonstrating reconfigurable magnetically-stable configurations, implementing autonomous control to generate these configurations, and further developing the theory to describe forces between modules and assemblies of modules. In addition, a more powerful electromagnet system will be created so that all disassembly methods can be computer controlled.

Acknowledgement

The authors would like to thank Brian Knight for use of the vibrating sample magnetometer, Magnequench, Inc. for graciously supplying us with magnetic powder, and the NanoRobotics Laboratory members for all of their support and suggestions. This work is supported by the National Science Foundation CAREER award program (NSF IIS-0448042), and the NSF Graduate Research Fellowship.

References

1. M. Yim, W.M. Shen, B. Salemi, D. Rus, M. Moll, H. Lipson, E. Klavins, G.S. Chirikjian, IEEE Robotics and Automation Magazine **14**, 43 (2007)
2. W.M. Shen, H. Chiu, M. Rubenstein, B. Salemi, in *Proceedings of the Space Technology International Forum* (Albuquerque, New Mexico, 2008)
3. S.C. Goldstein, J.D. Campbell, T.C. Mowry, Computer **38**, 99 (2005)
4. E. Yoshida, S. Kokaji, S. Murata, K. Tomita, H. Kurokawa, Journal of Robotics and Mechatronics **13**, 212 (2001)
5. B. Donald, C. Levey, I. Paprotny, Journal of Microelectromechanical Systems **17**, 789 (2008)
6. C. Pawashe, S. Floyd, M. Sitti, International Journal of Robotics Research (2009). In press
7. K. Vollmers, D. Frutiger, B. Kratochvil, B. Nelson, Applied Physics Letters **92** (2008)
8. O. Sul, M. Falvo, R. Taylor, S. Washburn, R. Superfine, Applied Physics Letters **89** (2006)
9. O. Ergeneman, G. Dogangil, M.P. Kummer, J.J. Abbott, M.K. Nazeeruddin, B.J. Nelson, IEEE Sensors Journal **8**, 2022 (2008)
10. S. Martel, O. Felfoul, J.B. Mathieu, A. Chanu, S. Tamaz, M. Mohammadi, M. Mankiewicz, N. Tabatabaei, International Journal of Robotics Research (2009). In press
11. B. Behkam, M. Sitti, Applied Physics Letters **90** (2007)
12. C. Pawashe, S. Floyd, M. Sitti, Applied Physics Letters **94** (2009)
13. S. Floyd, C. Pawashe, M. Sitti, IEEE Transactions on Robotics (2009). In press
14. Nanorobotics laboratory. http://nanolab.me.cmu.edu/projects/MagneticMicroRobot/
15. M. Imbaby, K. Jiang, I. Chang, Journal of Micromechanics and Microengineering **18** (2008)
16. D.K. Cheng, *Field and Wave Electromagnetics, 2nd Edition* (Addison-Wesley Publishing Company, Inc., 1992)
17. J. Israelachvili, *Intermolecular and Surface Forces* (Academic Press, 1992)